FGF21 mediates the lipid metabolism response to amino acid starvation

Ana Luísa De Sousa-Coelho,[*,†] Joana Relat,[*,†] Elayne Hondares,[†,§] Albert Pérez-Martí,[*,†] Francesc Ribas,[†,§] Francesc Villarroya,[†,§] Pedro F. Marrero,[*,†] and Diego Haro[1,*,†]

Departament de Bioquímica i Biologia Molecular,* Facultat de Farmàcia, Universitat de Barcelona, 08028 Barcelona, Spain; Institut de Biomedicina de la Universitat de Barcelona (IBUB),[†] 08028 Barcelona, Spain; and Departament de Bioquímica i Biologia Molecular,[§] Facultat de Biologia, Universitat de Barcelona and CIBER Fisiopatología de la Obesidad y Nutrición, 08028 Barcelona, Spain

Abstract Lipogenic gene expression in liver is repressed in mice upon leucine deprivation. The hormone fibroblast growth factor 21 (FGF21), which is critical to the adaptive metabolic response to starvation, is also induced under amino acid deprivation. Upon leucine deprivation, we found that FGF21 is needed to repress expression of lipogenic genes in liver and white adipose tissue, and stimulate phosphorylation of hormone-sensitive lipase in white adipose tissue. The increased expression of *Ucp1* in brown adipose tissue under these circumstances is also impaired in FGF21-deficient mice. Our results demonstrate the important role of FGF21 in the regulation of lipid metabolism during amino acid starvation.—De Sousa-Coelho, A. L., J. Relat, E. Hondares, A. Pérez-Martí, F. Ribas, F. Villarroya, P. F. Marrero, and D. Haro. **FGF21 mediates the lipid metabolism response to amino acid starvation. *J. Lipid Res*. 2013.** 54: **1786–1797.**

Supplementary key words brown adipose tissue • fibroblast growth factor 21 • leucine deprivation • liver • white adipose tissue

Amino acid starvation initiates a signal transduction cascade, starting with the activation of the general control nonderepressible 2 (GCN2) kinase, phosphorylation of eukaryotic initiation factor 2 (eIF2), and increased synthesis of activating transcription factor 4 (ATF4) (1). We have recently found that fibroblast growth factor 21 (*Fgf21*) is a target gene for ATF4. Consequently, FGF21 is induced by amino acid deprivation both in mouse liver and HepG2 cells as part of the transcriptional program initiated by increased levels of ATF4 (2).

FGF21 is a member of the FGF family with endocrine properties. It is predominantly produced by the liver, but is also produced by other tissues such as white adipose tissue (WAT), brown adipose tissue (BAT), skeletal muscle, and pancreas (3–6). FGF21 expression in liver is under tight control by peroxisome proliferator-activated receptor (PPAR) α (7–10). It is induced in the liver during fasting and its expression induces a metabolic state that mimics long-term fasting. Thus, FGF21 is critical for the induction of hepatic fat oxidation, ketogenesis, and gluconeogenesis, which are metabolic processes critical for the adaptive metabolic response to starvation (11). *Fgf21* is also a target of the liver X receptor that represses its induction during fasting (12, 13). Significantly, FGF21 extends life span in transgenic mice to a similar extent as dietary restriction (14).

A dietary amino acid imbalance alters metabolic pathways beyond protein homeostasis. GCN2-dependent inhibition of fatty acid synthase (FASN) activity, expression of lipogenic genes in liver, and increased mobilization of lipid stores occur in response to leucine deprivation in mice (15). In addition, the following have been observed: increased expression of β-oxidation genes, decreased expression of lipogenic genes and activation of FASN in WAT, and increased expression of uncoupling protein 1 (*Ucp1*) in BAT (16, 17).

This work was supported by the Ministerio de Educación y Ciencia (SAF2010-15217 to D.H. and SAF2011-23636 to F.V.) and the Ajut de Suport als Grups de Recerca de Catalunya (2009 SGR163). A.L.D.S-C. was supported by Fundação para a Ciência e a Tecnologia (FCT) from Portuguese Government.

Manuscript received 18 October 2012 and in revised form 6 May 2013.

Published, JLR Papers in Press, May 9, 2013
DOI 10.1194/jlr.M033415

Abbreviations: ACC1, acetyl-CoA carboxylase 1; β3AR, β3-adrenergenic receptor; ASNS, asparagine synthetase; ATF4, activating transcription factor 4; Atgl, adipose triglyceride lipase; BAT, brown adipose tissue; Cd36; cluster of differentiation 36; Cpt1a, carnitine palmitoyltransferase 1a; Ctl, control; DIO, diet-induced obesity; Dio2, type 2 deiodinase; eIF2, eukaryotic initiation factor 2; eWAT, epididymal white adipose tissue; Fabp4, fatty acid binding protein 4; FASN, fatty acid synthase; FGF21, fibroblast growth factor 21; FGFR1, fibroblast growth factor receptor 1; GCN2, general control nonderepressible 2; H and E, hematoxylin and eosin; HSL, hormone-sensitive lipase; KO, knockout; (−)leu, leucine-deficient; MAPK, mitogen-activated protein kinase; MEK, mitogen-activated protein/ERK kinase; PGC1, peroxisome proliferator-activated receptor γ coactivator 1; Plin1, perilipin 1; PPAR, peroxisome proliferator-activated receptor; qRT-PCR, quantitative RT-PCR; SREBP1c, sterol regulatory element binding protein 1c; Ucp1, uncoupling protein 1; WAT, white adipose tissue; WT, wild-type.

[1]To whom correspondence should be addressed.
e-mail: dharo@ub.edu.

The coincidence between the metabolic response to essential amino acid deprivation and to FGF21, the induction of *Fgf21* under amino acid deprivation (2), together with the repression of the transcription and maturation of sterol regulatory element binding protein 1c (SREBP1c) induced by FGF21 in HepG2 cells (18), led us to consider that FGF21 could be an important mediator between amino acid deprivation and lipid metabolism in liver, WAT, and BAT.

To investigate this hypothesis, we examined the response of FGF21-deficient mice to deprivation of the essential amino acid leucine. As expected, we found a huge increase in *Fgf21* expression in the liver of wild-type (WT) animals, along with a repression of lipogenic genes after 7 days of leucine deprivation. In this condition, FGF21-deficient mice developed liver steatosis caused by unrepressed expression of lipogenic genes. In WAT, the expression of lipogenic genes was also repressed and the phosphorylation of hormone-sensitive lipase (HSL) was increased under leucine deprivation. The absence of leucine also induced an increase in the expression of *Ucp1* and type 2 deiodinase (*Dio2*) in BAT. We found that all these effects in WAT and BAT were also impaired in FGF21-deficient mice. Here, we show the involvement of FGF21 in the regulation of lipid metabolism during amino acid starvation, thus reinforcing its important role as an endocrine factor in coordinating energy homeostasis under a variety of nutritional conditions.

MATERIALS AND METHODS

Animals and diets

Male WT and *Fgf21*-null mice (B6N; 129 S5-Fgf21tm1Lex/Mmucd), obtained from the Mutant Mouse Regional Resource Center, were housed in a temperature-controlled room (22 ± 1°C) on a 12/12 h light/dark cycle and were provided free access to commercial rodent chow and tap water prior to the experiments. Control (nutritionally complete amino acid) and leucine-deficient [(−)leu] diets were obtained from Research Diets, Inc. (New Brunswick, NJ). All diets were isocaloric and compositionally the same in terms of carbohydrate and lipid components. At the beginning of the feeding experiment, 12–15 week old male mice were first acclimated to the control diet for 7 days, and then randomly assigned to either the control diet group, with continued free access to the nutritionally complete diet, or the (−)leu diet group, with free access to the diet devoid of the essential amino acid leucine for 7 days. Food intake and body weight were recorded at least every 2 days. Animals were anesthetized by isoflurane inhalation, and blood was collected from the heart for the assay described below. After euthanization, tissues were isolated and immediately snap-frozen and stored at −80°C for future analysis. The Animal Ethics Committee of the University of Barcelona approved these experiments.

Cell culture and treatment conditions

HepG2 cells were cultured in Eagle's Minimal Essential Medium (MEM) (GIBCO, Invitrogen) supplemented to contain 1× nonessential amino acids, 4 mM glutamine, 100 μg/ml streptomycin sulfate, 100 units/ml penicillin G, and 10% (v/v) fetal bovine serum. Cells were maintained at 37°C in a 5% CO_2/95% air incubator, and cultures were replenished with fresh MEM medium and serum for approximately 16 h prior to initiating all treatments to ensure that the cells were in the basal ("fed") state. Amino acid deprivation was induced by transfer of cells to culture medium containing 2 mM histidinol (HisOH) for 8 h, which blocks charging of histidine onto the corresponding tRNA and thus mimics histidine deprivation and triggers activation of the AAR cascade (19). For mitogen-activated protein/ERK kinase (MEK) inhibition, the direct upstream kinases of ERK1/2, cells were treated with 30 μM PD98059 (PD98) for approximately 16 h before harvesting. HisOH (H6647) and PD98059 (P215) were purchased from Sigma-Aldrich (St. Louis, MO). Primary BAT adipocytes were obtained and maintained as previously described (20). Mouse 3T3-L1 adipocytes were cultured and differentiated as described previously (21).

Serum measurements. Serum was obtained by centrifugation of clotted blood and stored at −80°C. A mouse FGF21 enzyme-linked immunosorbent assay (ELISA) kit was obtained from Millipore for the quantification of FGF21 in mouse serum. The assay was conducted according to the manufacturer's protocol. Briefly, a calibration curve was constructed by plotting the difference in absorbance values at 450 and 590 nm versus the FGF21 concentrations of the calibrators, and concentrations of unknown samples (performed in duplicate) were determined using this calibration curve (22). The Veterinary Service of Clinical Biochemistry at the Universitat Autònoma de Barcelona determined blood biochemical parameters.

RNA isolation and relative quantitative RT-PCR. Total RNA was extracted from the frozen tissues [liver, epididymal white adipose tissue (eWAT), and BAT] or cells (3T3L1 and primary brown adipocytes) using TRI reagent solution (Ambion) followed by DNase I treatment (Ambion) to eliminate genomic DNA contamination. To measure the relative mRNA levels, quantitative (q)RT-PCR was performed using TaqMan reagents. cDNA was synthesized from 1 μg of total RNA by MLV reverse transcriptase (Invitrogen) with random hexamers (Roche Diagnostics) according to the manufacturer's instructions. TaqMan Gene Expression Master Mix and TaqMan Gene Expression assays (Invitrogen/Applied Biosystems) were used for the PCR step. Amplification and detection were performed using the Step-One Plus Real-Time PCR System. Each mRNA from a single sample was measured in duplicate, using 18S rRNA as an internal control. Results were obtained by the comparative threshold cycle (Ct) method and expressed as fold of the experimental control.

Protein extract preparation. Whole-cell lysates from HepG2 cells were isolated using NP40 lysis buffer [50 mM Tris-HCl (pH 8), 150 mM NaCl, 1% Nonidet P-40]. To obtain liver nuclear extracts, frozen liver was triturated within a mortar in liquid nitrogen and immediately homogenized with a Dounce homogenizer in 1 ml of HB buffer [15 mM Tris-HCl (pH 8), 15 mM NaCl, 60 mM KCl, 0.5 mM EDTA], and centrifuged at 800 *g* for 5 min. The resulting pellet was resuspended in 100 μl of HB buffer supplemented with 0.05% Triton X-100 (Sigma), and centrifuged for 10 min at 1,000 *g*. Nuclear pellets were washed with 1 ml of HB buffer supplemented with 0.05% Triton X-100 and 1 ml of HB buffer. Nuclei were incubated at 4°C for 30 min in 50 μl of HB buffer containing 360 mM KCl and centrifuged for 5 min at 10,000 *g*. The supernatant corresponding to the nuclear extract was collected, frozen, and stored at −80°C. To obtain liver, WAT, and BAT total extracts, tissues were homogenized in RIPA buffer and centrifuged at 12,000 *g* for 15 min at 4°C. The supernatant was collected and frozen at −80°C until analysis. Protein concentration was assayed using Bio-Rad reagent. All of the buffers were

supplemented with a mixture of protease inhibitors (Sigma-Aldrich), 0.1 mM phenylmethylsulfonyl fluoride (PMSF), and a phosphatase inhibitor cocktail (IPC3, Sigma-Aldrich).

Immunoblotting. Total and nuclear proteins were resolved by SDS-polyacrylamide gel electrophoresis and transferred onto a Hybond-P PVDF membrane (Millipore). Membranes were blocked for 1 h at room temperature. The blots were then incubated with primary antibody in blocking solution overnight at 4°C. Antibodies were diluted according to the manufacturer's instructions. The blots were washed three times and incubated with horseradish peroxidase-conjugated secondary antibody in blocking buffer for 2 h at room temperature. After three washes, the blots were developed using the EZ-ECL Chemiluminescence Detection Kit for HRP (Biological Industries). The quantification of phosphorylation was performed by densitometry of phosphorylated protein normalized to total protein using Image J software.

Antibodies. HSL (#4107), phospho HSL (#4126), ERK1/2 (#4695), phospho-ERK1/2 (#4370), and phospho-p38 (#9211) antibodies were purchased from Cell Signaling Technology. ATF4 (sc-200), p38α/β (A-12, sc-7972), and SREBP1c (C-20, sc-36) antibodies were from Santa Cruz Biotechnology, Inc. (Santa Cruz, CA); FASN (ab128870) antibody was from Abcam; acetyl-CoA carboxylase 1 (ACC1) (04-322) and phospho-ACC1 (07-303) antibodies were from Millipore; actin antibody (A2066) was from Sigma-Aldrich; and tubulin antibody (#CP06) was from Calbiochem.

Histological examinations. For the histological analysis, tissues (liver and eWAT) were fixed in 10% formalin (Sigma-Aldrich) and embedded in paraffin. Then, 4 μm thick sections were cut and stained with hematoxylin and eosin (H and E). Images were acquired using a Leica CTR 4000 microscope. Quantitative data were obtained using the IMAT program developed in the Science and Technology Center of the University of Barcelona. The selection of the test objects was performed according to color and choosing the same limits for binarization for all images. Adipocyte size and lipid accumulation were measured using at least three different randomly chosen fields of eWAT and liver sections, respectively, from each mouse.

Lipolysis assay. Lipolysis assay was performed after 24 h treatment with FGF21 using the Free Glycerol Determination Kit (Sigma).

Data analysis/statistics. All data are expressed as means ± SEM. Significant differences were assessed by a two-tailed Student's *t*-test. $P < 0.05$ was considered statistically significant. *a*, $P < 0.05$ versus control (Ctl) WT mice (or DMSO-treated HepG2 cells); *b*, $P < 0.05$ versus Ctl *Fgf21*-knockout (KO) mice; *c*, $P < 0.05$ versus (−)leu WT (or HisOH-treated HepG2 cells) (n = 6 per group of mice, or at least three independent experiments with HepG2 cells).

RESULTS

FGF21 gene expression is induced by leucine deprivation specifically in liver but not in BAT or WAT

According to our previously reported results (2), mice maintained on a (−)leu diet show a dramatic increase in FGF21 circulating levels (**Fig. 1A**). To check the origin of this circulating FGF21 we analyzed *Fgf21* gene expression in several tissues. Consistent with the liver as the main site of FGF21 production and release into the blood, *Fgf21* mRNA levels in liver paralleled those in serum, whereas mRNA levels were unchanged in BAT and, unexpectedly, significantly decreased in eWAT in WT mice maintained on a (−)leu diet (Fig. 1B). As expected, *Fgf21* mRNA levels were undetectable in any analyzed tissue in the *Fgf21*-KO mice. In accordance with previous reports (23), the circulating levels of FGF21 in KO mice were below the threshold for correct quantification.

FGF21 deficiency significantly attenuates weight loss under leucine deprivation

When fed a leucine-deprived diet, mice undergo rapid weight loss (16). The goal of the present study is to investigate whether this phenomenon is FGF21 dependent. For this purpose, WT and *Fgf21*-KO mice were fed a control or (−)leu diet for 7 days. Together with total body weight

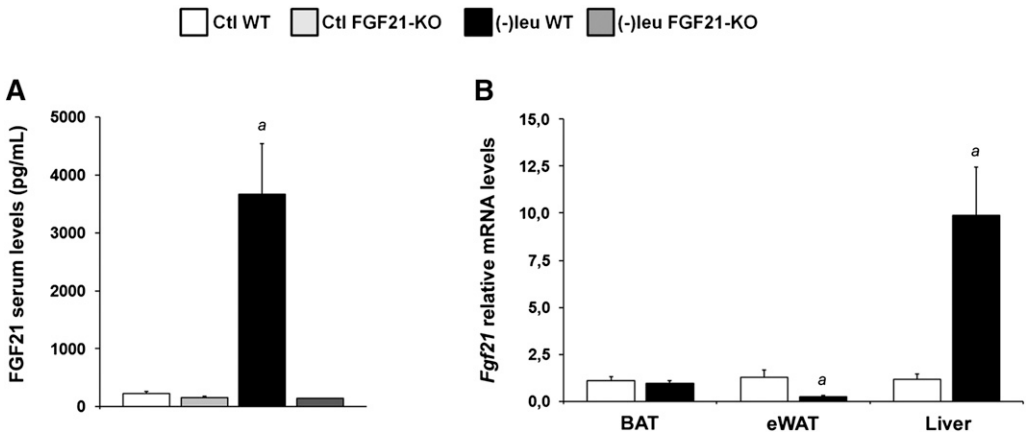

Fig. 1. FGF21 is differently regulated by leucine deprivation in liver and adipose tissues. A: Serum FGF21 protein concentrations were measured by ELISA. B: *Fgf21* mRNA in BAT, eWAT, and liver was measured by qRT-PCR. Error bars represent the mean ± SEM. *a*, $P < 0.05$ versus Ctl WT.

loss (**Figs. 2A, B**), mice fed a leucine-deprived diet undergo a fat mass loss, both epididymal and subcutaneous (Fig. 2D). We found that these effects were partially blunted in *Fgf21*-KO mice (Figs. 2A, B, D), while the reduction in food intake caused by leucine deprivation (~30%) was unchanged between genotypes (Fig. 2C).

The reported observation that white adipocytes from FGF21 transgenic mice are substantially smaller than those from WT mice (8, 24) and that leucine deprivation decreased adipocyte volume (16), led us to examine whether this effect was FGF21 dependent. A histological analysis of eWAT (**Fig. 3A**) showed that leucine deprivation resulted in a reduction in adipocyte volume compared with mice fed a control diet. By contrast, the adipocyte volume was only slightly reduced in (−)leu-fed *Fgf21*-KO mice and remained unchanged in *Fgf21*-KO mice on the control diet (Fig. 3A). We note that other groups reported increased (25) or decreased (26) adipocyte size in *Fgf21*-KO mice on regular diets. We have no explanation for these discrepancies beyond potential minor differences in the composition of the diet.

Increased phosphorylation of HSL under leucine deprivation is FGF21 dependent

It has been previously described that leucine deprivation increases lipolysis in WAT (16). It has also been suggested that FGF21 stimulates lipolysis in WAT during normal feeding, but inhibits it during fasting (25). Therefore, to examine the role of FGF21 in lipolysis, we evaluated the mRNA levels of adipose triglyceride lipase (*Atgl*), *Hsl*, and perilipin 1 (*Plin1*), and the levels of phosphorylated HSL. We did not find any statistically significant changes in *Atgl*, *Hsl*, or *Plin1* mRNA levels upon leucine deprivation (Fig. 3B). Consistent with changes in body weight, lack of FGF21 significantly decreased levels of phosphorylated HSL in WAT under leucine deprivation (Fig. 3C), which suggests that lipolysis was impaired in these mice. Despite the evidence of increased lipolysis under leucine deprivation, levels of free fatty acids in serum were not significantly altered in the conditions analyzed (**Table 1**), suggesting increased fatty acid utilization by other tissues.

FGF21 deficiency prevents changes in liver and WAT in leucine-deprived mice

A link between FGF21 and SREBP1c during lipogenesis in cultured hepatocytes has recently been proposed (18). As lipogenic genes are downregulated in the liver of mice deprived of leucine (15), we speculated that FGF21 might regulate their expression. To investigate this possibility, we examined the expression of genes involved in the regulation of lipid metabolism in the liver

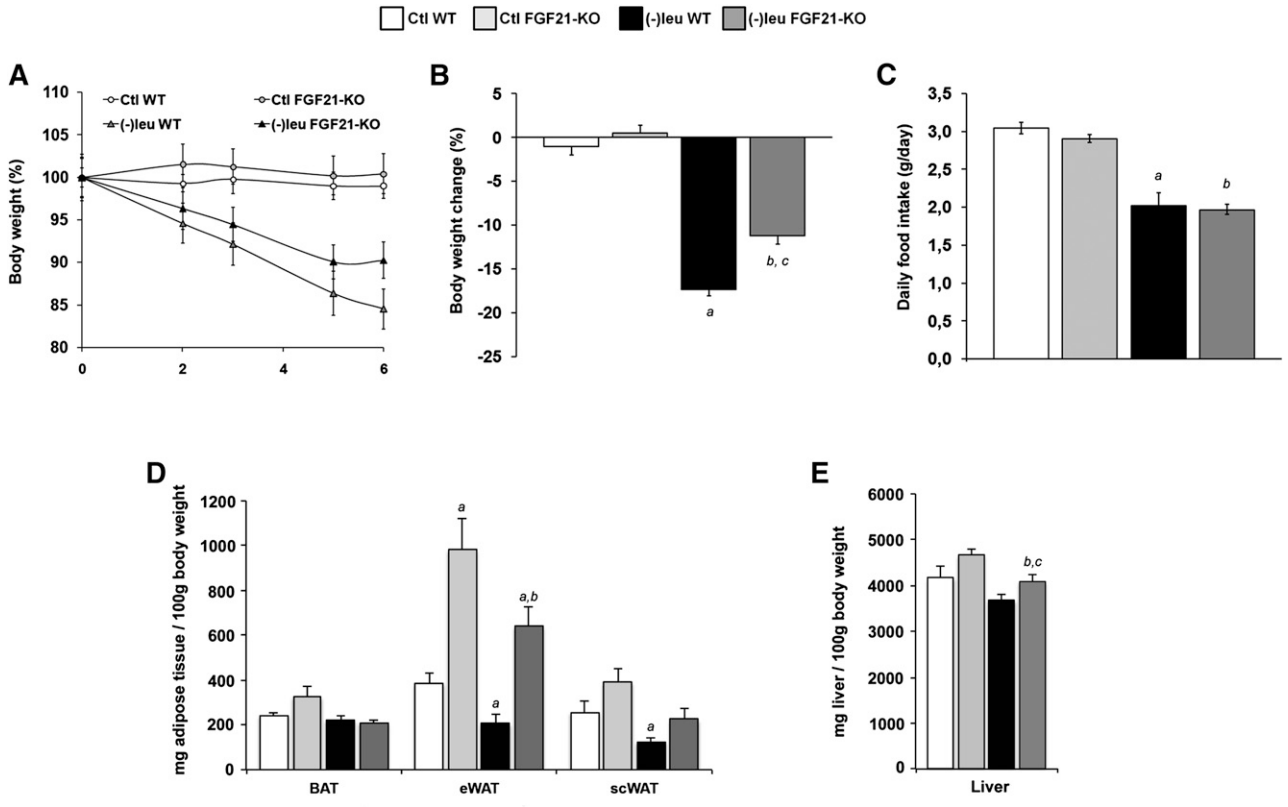

Fig. 2. FGF21 is required for (−)leu diet effects on body weight without affecting food consumption. A: Body weight of mice fed with Ctl or (−)leu diet. The weight on the first day was considered 100%. B: Body weight change (%) after 7 days of feeding the Ctl or (−)leu diet. C: Daily food intake. D: BAT, eWAT, and scWAT weight of mice fed with Ctl or (−)leu diet related to 100 mg of body weight. E: Liver weight of mice fed with Ctl or (−)leu diet related to 100 mg of body weight. Error bars represent the mean ± SEM. *a*, $P < 0.05$ versus Ctl WT mice; *b*, $P < 0.05$ versus Ctl FGF21-KO mice; *c*, $P < 0.05$ versus (−)leu WT mice (n = 6/group).

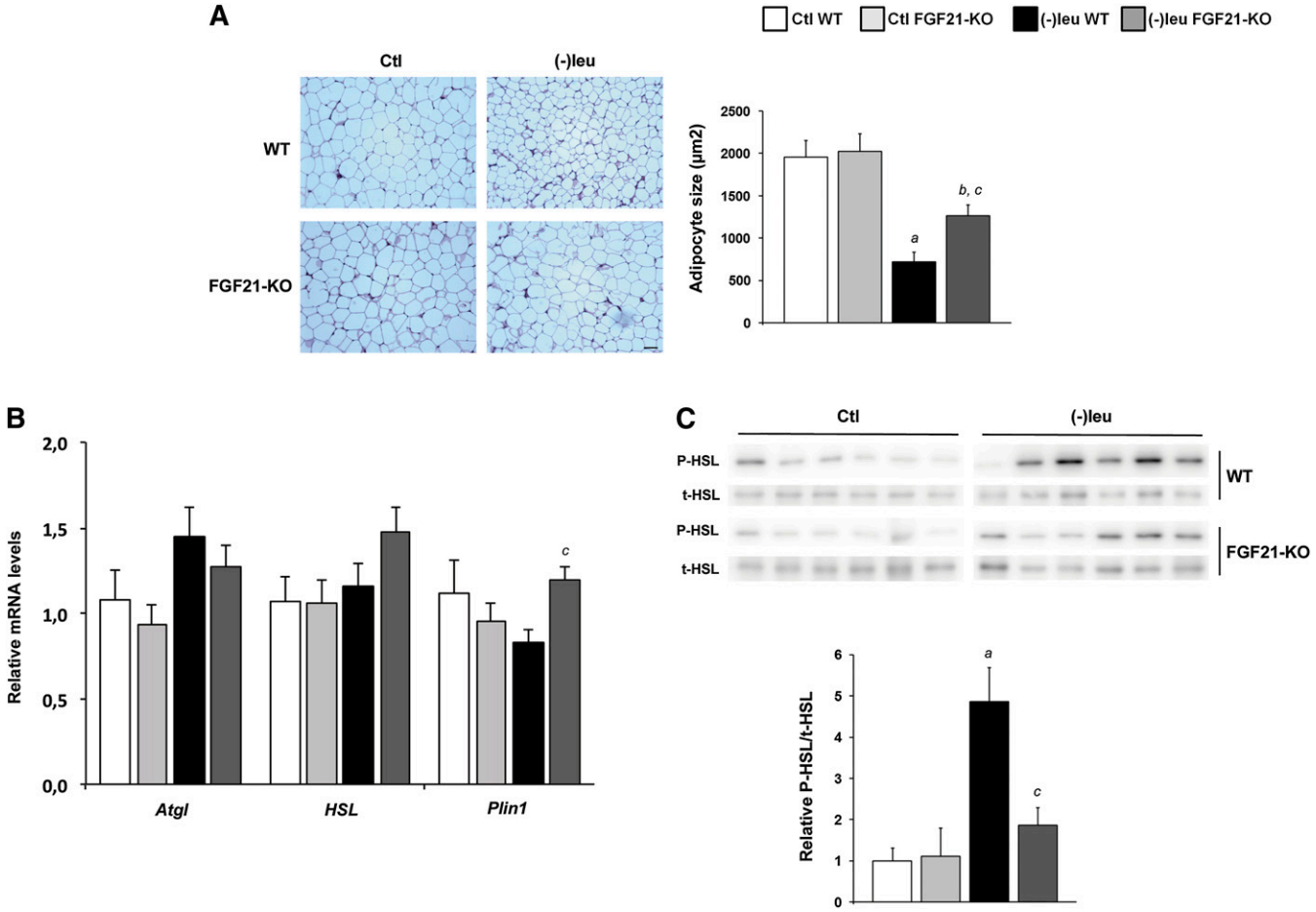

Fig. 3. The (−)leu diet effects on adipocyte size and lipid metabolism in WAT are FGF21 dependent. A: Representative H and E-stained eWAT sections from WT and FGF21-KO mice (×20 magnification). Scale bar, 50 µM. Adipocyte size (right panel) was measured as described in Materials and Methods, using at least three different randomly chosen fields of eWAT sections from each mouse. B: *Atgl*, *Hsl*, and *Plin1* gene expression was measured by qRT-PCR in mouse eWAT. C: Phosphorylated HSL (P-HSL) and total HSL (t-HSL) protein levels were measured in WT and FGF21-KO eWAT homogenates by Western blot analysis. The bottom panel shows quantification by densitometry of phosphorylated HSL normalized to total HSL using Image J software. Error bars represent the mean ± SEM. *a*, $P < 0.05$ versus Ctl WT mice; *b*, $P < 0.05$ versus Ctl FGF21-KO mice; *c*, $P < 0.05$ versus (−)leu WT mice (n = 6/group). P-HSL, phosphorylated HSL.

of WT and *Fgf21*-KO mice maintained either on the control or (−)leu diet. As expected, levels of *Fasn*, *Srebp1c*, and *Acc1* mRNA were significantly decreased on the (−)leu diet. However, in mice lacking FGF21, the reduced expression of *Fasn* was statistically significantly increased, and, although not statistically significant, showed a tendency to increase in both *Srebp1c* and *Acc1* (**Fig. 4A**). The expression of other genes involved in fatty acid uptake [cluster of differentiation 36 (*Cd36*) and fatty acid binding protein 4 (*Fabp4*)] or oxidation [carnitine palmitoyltransferase 1a (*Cpt1a*)] was decreased in the absence of *Fgf21*. The analysis of FASN, SREBP1c, and ACC1 protein abundance showed a good correlation with the gene expression data (Fig. 4B). By contrast ACC1 phosphorylation was decreased under leucine deprivation in both WT and *Fgf21*-KO mice.

TABLE 1. Serum measurements in mice maintained on different diets

	WT Ctl	FGF21-KO Ctl	WT leu(−)	FGF21-KO leu(−)
NEFA (nmol/l)	0.79 ± 0.11	1.05 ± 0.11	0.73 ± 0.09	0.82 ± 0.06
TG (mg/dl)	95.79 ± 7.18	153.73 ± 11.62[a]	99.39 ± 15.36	186.08 ± 27.38[a,c]
Cholesterol (mg/dl)	101.13 ± 13,13	147.65 ± 4.21[a]	96.40 ± 7.69	122.55 ± 3.08[b,c]
Glucose (mg/dl)	209.43 ± 10.45	212.90 ± 7.88	185.53 ± 14.87	187.02 ± 9.55
Glycerol (µmol/l)	393.50 ± 38.32	520.95 ± 23.10[a]	313.93 ± 26.56	372.16 ± 19.99[b]
Insulin (µg/l)	1.26 ± 0.23	2.01 ± 0.52	0.41 ± 0.04[a]	1.21 ± 0.20[c]

All data are expressed as means ± SEM. Significant differences were assessed by a two-tailed Student's *t*-test. $P < 0.05$ was considered statistically significant. n = 6/group of mice. TG, triglycerides.

[a] $P < 0.05$ versus Ctl WT mice.

[b] $P < 0.05$ versus Ctl FGF21-KO mice.

[c] $P < 0.05$ versus (−)leu WT mice.

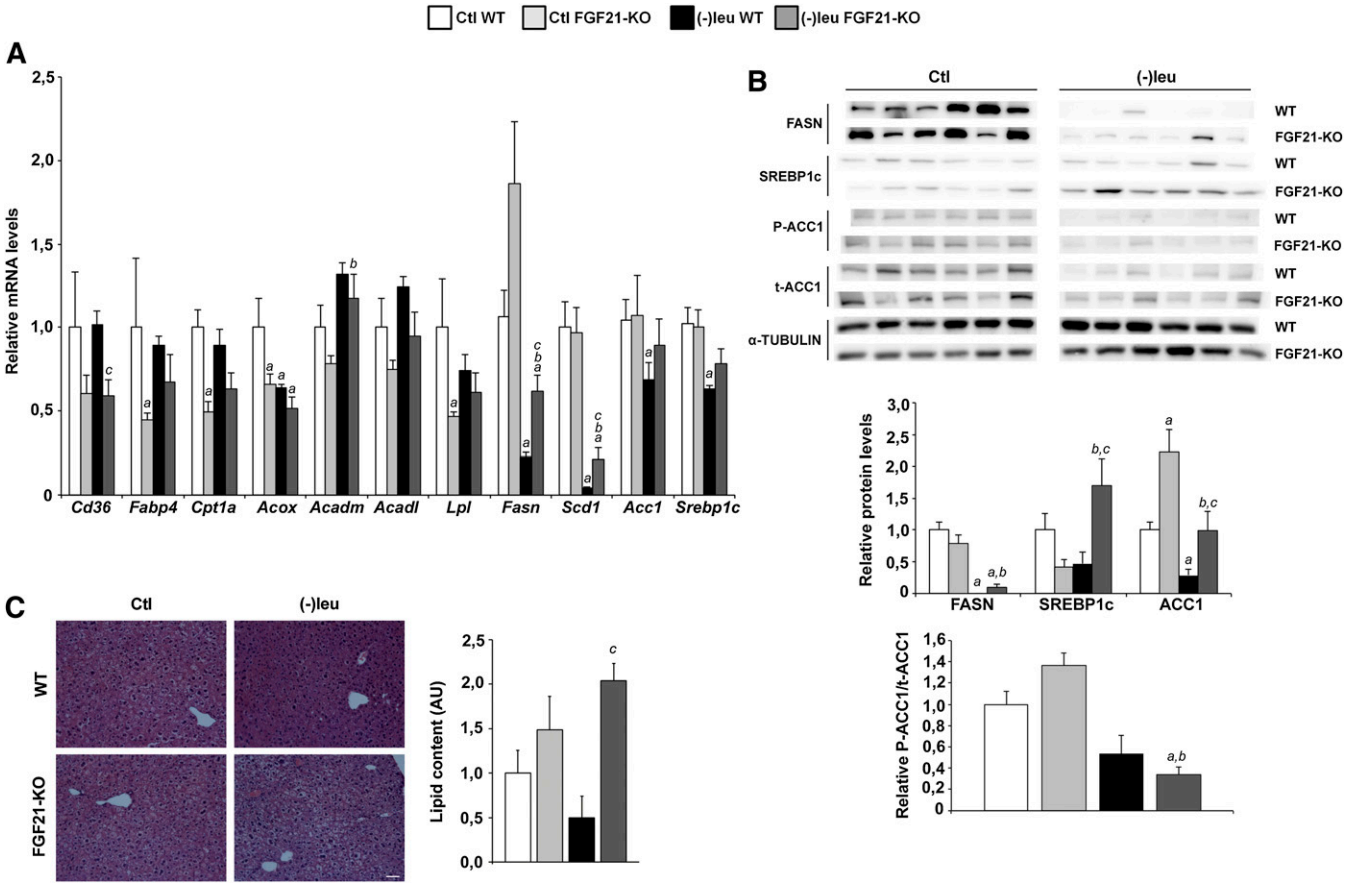

Fig. 4. FGF21-KO liver has impaired lipid metabolism and lipid accumulation in response to leucine deprivation. A: Expression of genes related with lipid handling was measured by qRT-PCR in mouse liver. B: FASN, SREBP1c, phosphorylated ACC1 (P-ACC1), and total ACC1 (t-ACC1) protein levels were detected by Western blot analysis in mouse liver. The bottom panel shows quantification by densitometry of the immunoblotted proteins using Image J software. Error bars represent the mean ± SEM. *a*, $P < 0.05$ versus Ctl WT mice; *b*, $P < 0.05$ versus Ctl FGF21-KO mice; *c*, $P < 0.05$ versus (−)leu WT mice (n = 6/group). C: Histological appearance and hepatic lipid accumulation of H and E liver staining of WT and FGF21-KO mice maintained either on a Ctl or a (−)leu diet. Representative H and E-stained hepatocytes are shown (×20 magnification). Scale bar, 50 μM. Lipid accumulation (right panel) was measured as described in Materials and Methods, using at least three different randomly chosen fields of liver sections from each mouse. Acadm, medium-chain acyl-CoA dehydrogenase; Acadl, long-chain acyl-CoA dehydrogenase; Acox, acetyl-CoA oxidase; Lpl, lipoprotein lipase; Scd1, stearoyl-CoA desaturase 1.

Although liver triglyceride levels, measured by extraction and posterior quantification, did not reflect the expression pattern of the lipid synthesis genes, H and E staining revealed it. This suggested a decreased lipid accumulation under leucine deprivation in WT animals that does not seem to occur in the *Fgf21*-KO mice (Fig. 4C).

As expected, gene expression analysis in eWAT revealed that the mRNA levels of the lipogenic genes *Fasn*, *Srebp1c*, and *Acc1* were also lower in this tissue in mice maintained on the (−)leu diet. These changes were blunted in the *Fgf21*-KO mice, particularly for *Fasn* (**Fig. 5A**). The analysis of FASN protein abundance showed a good correlation with the gene expression data (Fig. 5B).

We have analyzed the expression of the FGF21-receptor complex β-Klotho and fibroblast growth factor receptor 1 (FGFR1) in WAT. There was a significant increase in both β-Klotho and *Fgfr1* mRNA levels induced by both *Fgf21* knockout and leucine deprivation (Figs. 5C).

To further confirm the results obtained in mice, we have analyzed the expression of lipogenic and lipolytic genes in 3T3L1 treated with FGF21. This treatment induced a decrease in the expression of *Fasn*, *Srebp1c*, and *Acc1* and also of *Atgl* and *Plin* (Fig. 5D).

The FGF21-dependent phenotype during leucine deprivation is not related with the mitogen-activated protein kinase ERK1/2 signaling pathway

As described, mitogen-activated protein kinase (MAPK) ERK1/2 signaling is required for the amino acid starvation response (27, 28). Accordingly, histidinol treatment of HepG2 cells, which blocks charging of histidine onto the corresponding tRNA and thus mimics histidine deprivation, induced the phosphorylation of ERK1/2 (**Fig. 6A**). In addition, increased *FGF21* and asparagine synthetase (*ASNS*), mRNA levels (Fig. 6C), as well as increased ATF4 protein levels in HisOH-treated cells (Fig. 6B) were reduced in the presence of the MEK inhibitor PD98. In these cells, *FASN* expression is opposed to that of *FGF21* (Fig. 6D), mimicking what we observed in leucine-deprived WT (high FGF21) or *Fgf21*-null mice (Fig. 4A).

As it has been described that exogenous FGF21 is able to induce ERK1/2 phosphorylation in the liver and WAT

JOURNAL OF LIPID RESEARCH

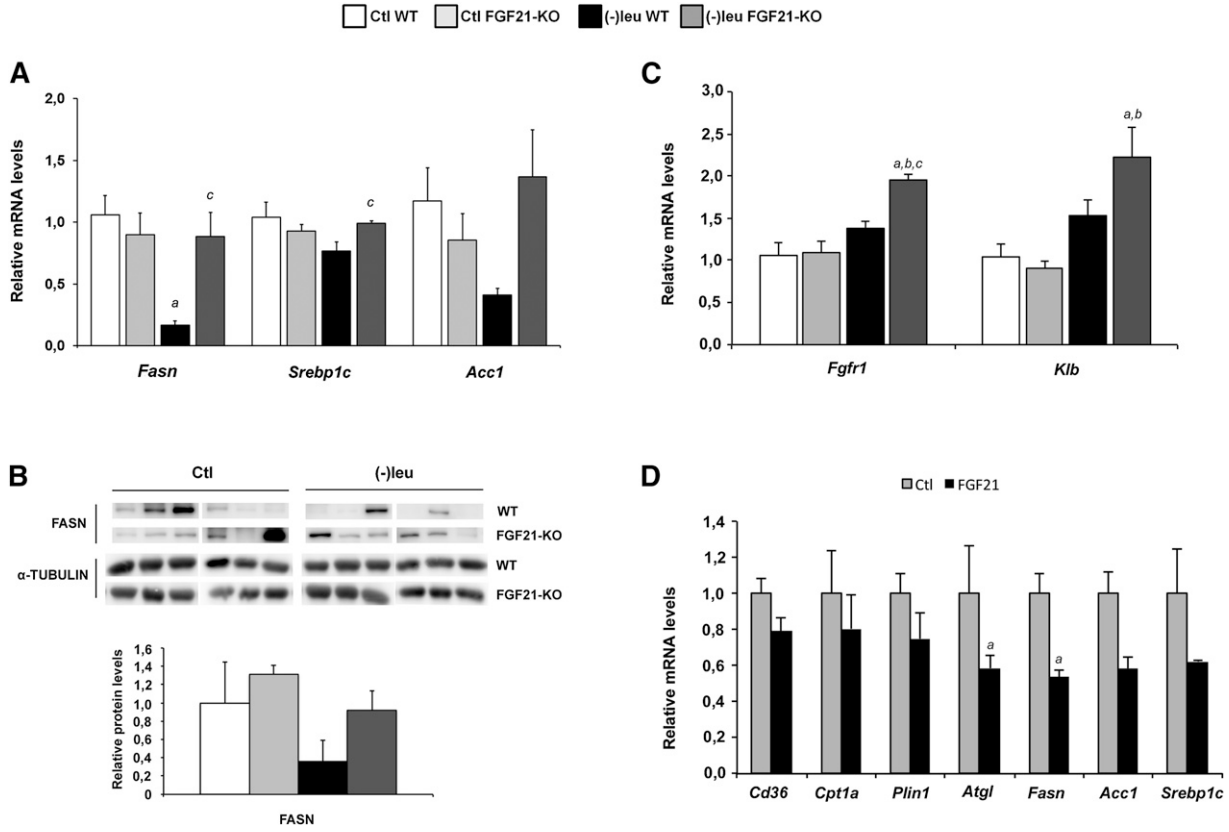

Fig. 5. FGF21-KO eWAT has altered lipogenic pathway in response to leucine deprivation. A: *Fasn*, *Srebp1c*, and *Acc1* gene expression was measured by qRT-PCR in mouse eWAT. B: FASN protein levels were detected by Western blot analysis in mouse liver. The bottom panel shows quantification by densitometry of the immunoblotted proteins using Image J software. Error bars represent the mean ± SEM. *a*, $P < 0.05$ versus Ctl WT mice; *b*, $P < 0.05$ versus Ctl FGF21-KO mice; *c*, $P < 0.05$ versus (−)leu WT mice (n = 6/group). C: *FgfR1* and β-Klotho gene expression was measured by qRT-PCR in mouse eWAT. D: The expression of genes related with lipid metabolism pathways was measured by qRT-PCR in 3T3L1 adipocytes treated with recombinant FGF21 (100 nM) for 24 h. Error bars represent the mean ± SEM. *a*, $P < 0.05$ versus Ctl WT mice; *b*, $P < 0.05$ versus Ctl FGF21-KO mice; *c*, $P < 0.05$ versus (−)leu WT mice (n = 6/group).

of acutely treated mice (29); we checked ERK1/2 phosphorylation in leucine-deprived WT and FGF21-null mice. Effectively, ERK1/2 phosphorylation was induced in the liver of leucine-deprived mice, although there were no differences between genotypes (Fig. 6E). Accordingly, the amino acid starvation response program was correctly initiated in *Fgf21*-KO mice, as shown by the increased levels of ATF4 protein and *Asns*, a prototypical ATF4 target gene, mRNA levels (Fig. 6F). Moreover, despite the fact that FGF21 serum levels are highly increased in leucine-deprived mice (Fig. 1A), ERK1/2 phosphorylation is not modified in WAT (Fig. 6G).

FGF21 deficiency prevents increases in BAT activation in leucine-deprived mice

Thermogenesis in BAT is mediated by the upregulation of UCP1 (30). It has been proposed that the induction of FGF21 production by the liver mediates direct activation of brown fat thermogenesis during the fetal-to-neonatal transition (20). FGF21 also regulates PPARγ coactivator 1 (PGC1) α and browning of WAT in adaptive thermogenesis (31). Consistent with previous results (16), leucine deprivation increased levels of *Ucp1* and *Dio2* mRNAs in the BAT of WT mice. These changes were blocked in *Fgf21*-KO mice (**Fig. 7A**). Because UCP1 expression is related to energy expenditure, the absence of induction of *Ucp1* in *Fgf21*-KO mice under leucine deprivation may contribute to the decrease in weight loss observed under these circumstances. mRNA levels of *Pgc1α*, which regulates the expression of UCP1 (32), were also increased. However, they did not differ between WT and *Fgf21*-KO mice under either control or (−)leu diet conditions (Fig. 7B). The same pattern as for *Pparγ* and *Pgc1α* was observed for *Adrb3* mRNA levels (Fig. 7C). We tested the possibility that the activation of p38 MAPK by the β3-adrenergic receptor (β3AR) participated in the induction of the *Ucp1* gene in BAT under this situation. However, although p38 phosphorylation, but not PKA activity, is induced in primary brown adipocytes treated with recombinant FGF21 (data not shown), phosphorylated p38 levels remained unchanged between diets and genotypes in BAT (Fig. 7C).

We have also analyzed the expression of lipogenic and lipolytic genes and glycerol release in primary brown adipocytes treated with FGF21. This treatment decreased the expression of *Fasn* and increased glycerol release without significant changes in the expression of *Atgl* and *Plin*

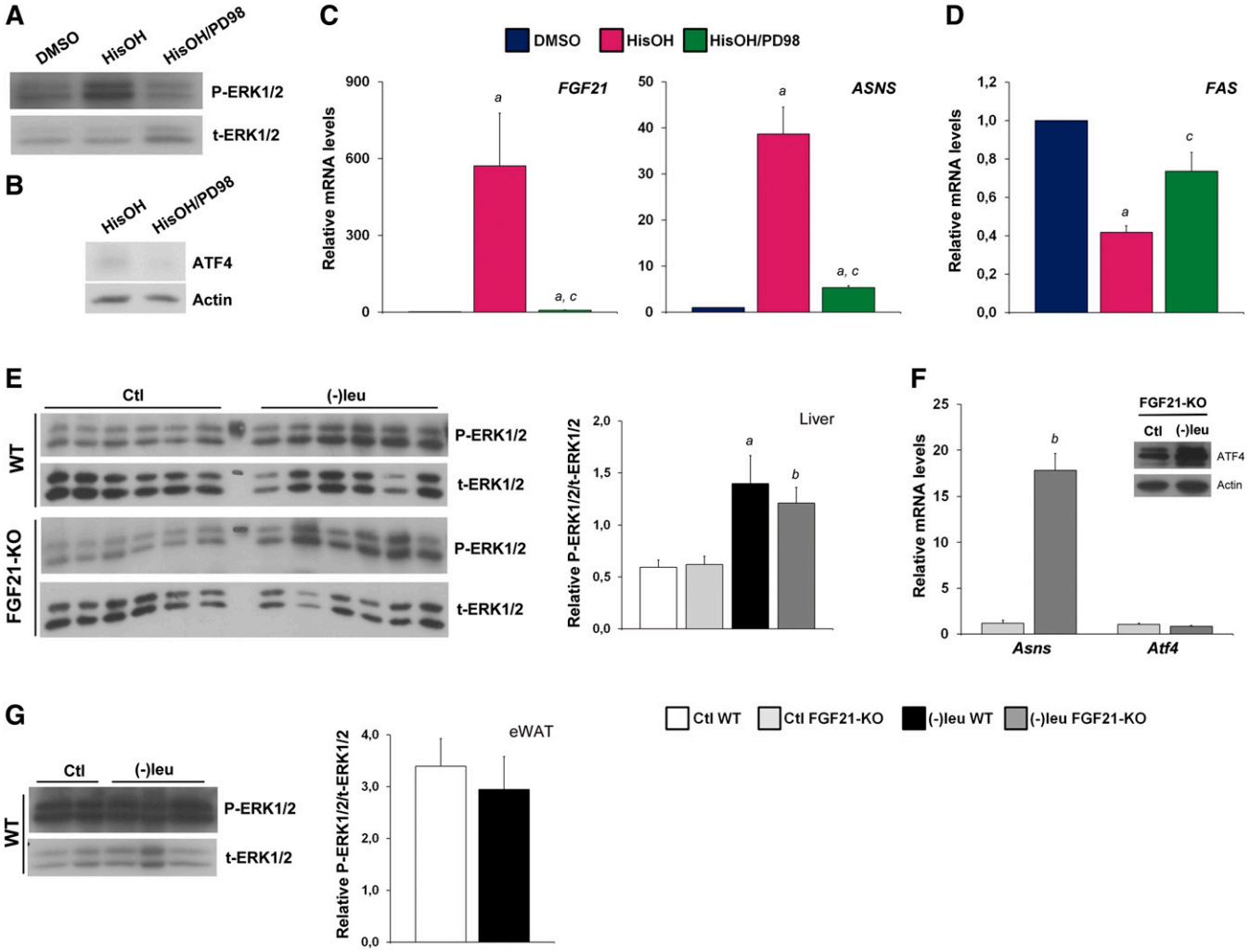

Fig. 6. Activation of the MEK/ERK pathway in the liver by leucine deprivation is independent of FGF21. HepG2 cells were incubated for 8 h with HisOH (2 mM) and the MEK inihibitor PD98 (30 μM), when indicated. Phosphorylation of ERK1/2 (A) and ATF4 protein levels (B) were analyzed by Western blot in total and nuclear HepG2 extracts, respectively. mRNA levels for *FGF21*, *ASNS* (C), and *FASN* (D) were analyzed by qRT-PCR. E: Phosphorylated ERK1/2 (P-ERK1/2) and total ERK1/2 (t-ERK1/2) levels were measured in liver extracts of WT and FGF21-KO mice by Western blot analysis. The right panel shows quantification by densitometry of phosphorylated ERK1/2 normalized to total ERK1/2 using Image J software. F: *Asns* and *Atf4* mRNA levels and nuclear ATF4 protein levels (insert), were measured in FGF21-KO mouse liver by qRT-PCR and Western blot, respectively. Actin was used as a loading control. A representative blot is shown. G: Phosphorylated and total ERK1/2 levels were measured in WT mouse eWAT homogenates by Western blot analysis. The right panel shows quantification by densitometry of phosphorylated ERK1/2 normalized to total ERK1/2 using Image J software. Error bars represent the mean ± SEM. *a*, $P < 0.05$ versus Ctl WT mice; *b*, $P < 0.05$ versus Ctl FGF21-KO mice; *c*, $P < 0.05$ versus (−)leu WT mice (n = 6/group).

(Fig. 7E, F). Accordingly, mRNA levels of *Hsl* and *Atgl* as well as HSL phosphorylation did not change in BAT of *Fgf21*-deficient mice (Fig. 7B, D).

DISCUSSION

We have previously shown that leucine deprivation significantly increased FGF21 hepatic expression and serum protein levels (2), suggesting an important role of this hormone in the amino acid starvation phenotype. In the current study, we demonstrate that in response to leucine deprivation, weight loss, downregulation of liver and WAT key lipogenic genes, as well as BAT activation are partly FGF21 dependent. Our results show that the FGF21 serum levels positively correlate with the mRNA levels measured in liver but not in BAT or WAT where they were not affected or even downregulated.

We have seen that FGF21 deficiency significantly attenuates weight loss under leucine deprivation; although the established reduction in food intake induced by a leucine-deprived diet was not changed by the absence of FGF21. This means that FGF21 is in part responsible for the loss of weight under amino acid deprivation, independently of food intake. Consistent with our observation, previous studies have shown that FGF21 transgenic mice are resistant to diet-induced obesity (DIO) and that FGF21 treatment induced weight loss in genetically obese (ob/ob) mice (24, 33, 34).

It has been shown that white adipocytes from FGF21 transgenic mice are substantially smaller than those from WT mice (8, 24). Here, we demonstrate that the reduction

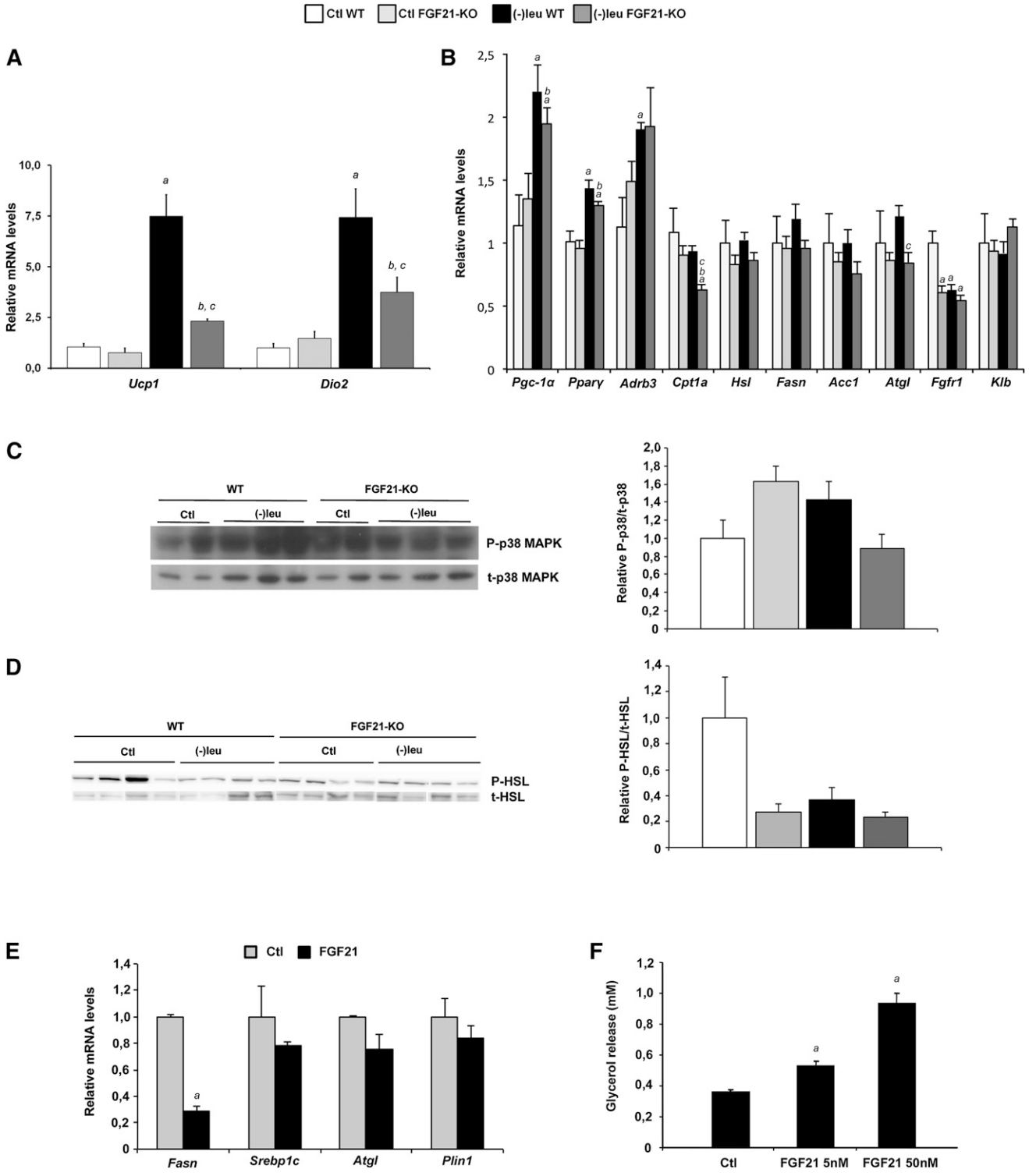

Fig. 7. FGF21 is required for inducing BAT activation during amino acid deprivation. A: *Ucp1* and *Dio2* gene expression was measured by qRT-PCR in mouse BAT. B: The expression of genes related with lipid metabolism was measured by qRT-PCR in mouse BAT. C: Phosphorylated p38 MAPK (P-p38 MAPK) and total p38 MAPK (t-p38 MAPK) levels were measured in WT and FGF21-KO mouse liver extracts by Western blot analysis. The right panel shows quantification by densitometry of phosphorylated p38 MAPK normalized to total p38 MAPK using Image J software. D: Phosphorylated and total HSL protein levels were measured in WT and FGF21-KO eWAT homogenates by Western blot analysis. The right panel shows quantification by densitometry of phosphorylated HSL normalized to total HSL, using Image J software. A representative blot is shown. E: *Fasn, Srebp1c, Atgl* and *Plin1* gene expression was measured by qRT-PCR in differentiated primary BAT treated with FGF21 (50nM) for 24h. F: Glycerol release in differentiated primary BAT treated with FGF21 (5nM and 50nM) for 24h. Error bars represent the mean ± standard error of the mean (SEM). Error bars represent the mean ± SEM. A representative blot is shown. *a*, $P < 0.05$ versus Ctl WT mice; *b*, $P < 0.05$ versus Ctl FGF21-KO mice; *c*, $P < 0.05$ versus (−)leu WT mice (n = 6/group).

in the adipocyte volume that occurs under leucine deprivation depends on the increased FGF21 expression and secretion that takes place under this diet.

We have found that the levels of phosphorylated (P)-HSL were increased upon (−)leu feeding in eWAT, as it was described in (16), so activation of the HSL protein probably allowed increased lipolysis. Interestingly, our results show that lack of FGF21 significantly decreases phosphorylated HSL levels in the eWAT of (−)leu-fed mice, suggesting an important role of FGF21 action on leucine deprivation-induced lipolysis.

The analysis of blood biochemical parameters, however, did not show significant changes in NEFA levels, likely due to increased fatty acid utilization by other tissues. We assume that there is an increased glucagon signaling under leucine deprivation, indicated by the increased PKA-dependent HSL Ser660 phosphorylation in WAT. Additionally, a reduction in insulin levels under leucine deprivation is observed in WT but not in KO mice; these changes are well correlated with the differences observed in body weight and fat mass.

We have also examined whether the impaired reduction in body weight observed in *Fgf21*-KO mice under leucine deprivation was not only related to lipolysis in WAT, but also to other factors that influence adipose tissue mass as lipogenesis. We have observed a significant reduction in *Fasn* mRNA levels in eWAT upon (−)leu feeding that was totally blocked in *Fgf21*-KO mice. *Srebp1c* and *Acc1* mRNA levels presented the same pattern, although with distinct statistical significances. The endocrine effect of FGF21 on WAT under leucine deprivation that we observe here is different from the recently described autocrine effect on this tissue in a fed state, in which FGF21 induces lipogenesis through the regulation of PPARγ activity (26). The decreased *Fgf21* expression in WAT under leucine deprivation also contrasts with its observed induction after one day of fasting (35). FGF21 administration to DIO mice leads to a dramatic decrease in the WAT *Fgf21* transcript. However, controversially, it induces an increase in the expression of adipogenic genes (33). It seems, therefore, that the response to increased levels of FGF21 depends on its origin and other factors, which may reflect the metabolic state and the energy requirements of the organism.

An inhibitory action in the lipid synthesis had been already described for FGF21 (36). It was demonstrated that the reduction of hepatic triglyceride levels was associated with FGF21 inhibition of nuclear sterol regulatory element binding protein 1c (*Srebp1c*) and the expression of an extended array of genes involved in fatty acid and triglyceride synthesis. Accordingly, in liver, we have seen that the expected reduction in the mRNA levels of *Srebp1c*, *Fasn*, and *Acc1* by (−)leu diet was not observed in *Fgf21*-KO mice. We have also seen a direct effect in lipogenic gene expression in both 3T3L1 cells and primary brown adipocytes treated with recombinant FGF21.

The induction, in liver from *Fgf21*-KO mice, of *Asns* expression, for which the gene product catalyzes the glutamine and ATP-dependent conversion of aspartic acid to asparagine, suggests that FGF21 is not involved in the control of amino acid metabolism under amino acid starvation. We have also observed that contrary to the exogenous FGF21 induction of ERK1/2 phosphorylation in the liver and WAT of acutely treated mice (29), the FGF21-dependent phenotype in leucine deprivation is unexpectedly not related with the MAPK ERK1/2 signaling pathway both in liver and WAT.

BAT is a major site of adaptive thermogenesis, and it is used to preserve both thermal and caloric homeostasis in response to environmental temperature or diet (37). *Fgf21*-KO mice under leucine deprivation exhibited decreased induction of genes defining BAT identity (i.e., *Ucp1* and *Dio2*), while its transcriptional regulators *Pgc1α* and *Pparγ* were identically induced in both WT and *Fgf21*-KO mice. Increased *Ucp1* expression may be regulated by the sympathetic nervous system through the activation of β-adrenergic receptors. We found that the mRNA expression of *Adrb3* was induced by leucine deprivation in BAT, although there were no significant changes between genotypes. The β3AR stimulates p38 MAPK, which is required for the βAR-dependent increase in *Ucp1* expression in brown adipocytes (38). Nevertheless, p38 phosphorylation levels were not affected by leucine deprivation compared with control, both in the WT

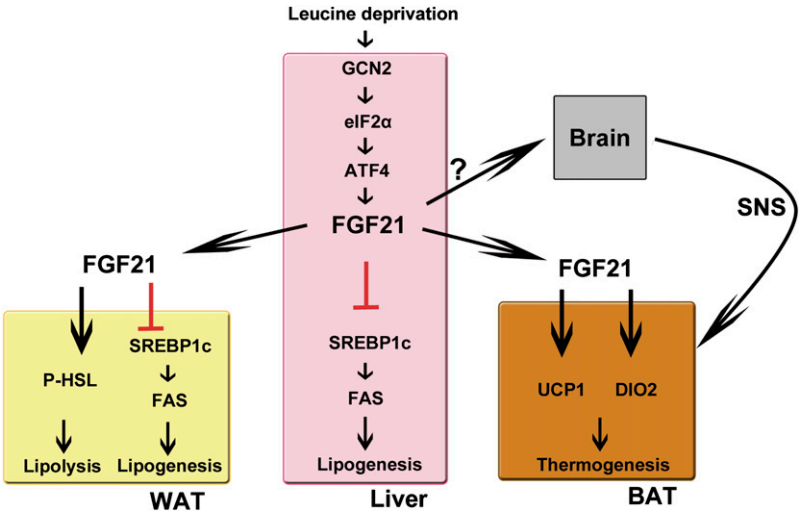

Fig. 8. Working model of the FGF21 regulatory pathway under leucine deprivation.

and *Fgf21*-KO mice. One of the best-known inducers of BAT and its function is norepinephrine (39), which has also been shown to be induced in leucine-deprived mice (16). These findings raise the possibility that FGF21 might induce *Ucp1* (and also *Dio2*) through an indirect mechanism involving the central nervous system. Of interest, it has been recently proposed that increased expression of FGF21 secreted from liver enters the brain and stimulates the hypothalamic-pituitary-adrenal axis (40). However, a more extensive analysis of other candidate factors should be performed in the future, and further investigation will be required to determine the exact mechanism by which FGF21 induces BAT activation.

In summary, we found that FGF21 is an important factor, although not the only one, in mediating the changes in lipid metabolism observed upon leucine deprivation (**Fig. 8**). We have shown that *Fgf21*-deficient mice under these circumstances showed unrepressed lipogenesis in liver and WAT, decreased phosphorylation of HSL in WAT indicating impaired lipolysis, and impaired induction of *Ucp1* expression in BAT. Thus, our results suggest that FGF21 plays an important role in the regulation of lipid metabolism during amino acid starvation.

While this work was under revision, a study was published (41) that showed the Atf4-dependent induction of FGF21 in mice with autophagy deficiency in skeletal muscle or liver. As a result of this induction, these mice are protected from diet-induced obesity and insulin resistance. In the supplementary results of this paper, the authors confirm that the ATF4-FGF21 axis also has a physiologically relevant role under conditions of leucine deprivation. In agreement with our results, they also show how the effects of leucine deprivation on body weight, fat weight, and blood glucose are partially diminished in *Fgf21*-KO mice.

REFERENCES

1. Kilberg, M. S., J. Shan, and N. Su. 2009. ATF4-dependent transcription mediates signaling of amino acid limitation. *Trends Endocrinol. Metab.* **20:** 436–443.
2. De Sousa-Coelho, A. L., P. F. Marrero, and D. Haro. 2012. Activating transcription factor 4-dependent induction of FGF21 during amino acid deprivation. *Biochem. J.* **443:** 165–171.
3. Nishimura, T., Y. Nakatake, M. Konishi, and N. Itoh. 2000. Identification of a novel FGF, FGF-21, preferentially expressed in the liver. *Biochim. Biophys. Acta.* **1492:** 203–206.
4. Johnson, C. L., J. Y. Weston, S. A. Chadi, E. N. Fazio, M. W. Huff, A. Kharitonenkov, A. Köester, and C. L. Pin. 2009. Fibroblast growth factor 21 reduces the severity of cerulein-induced pancreatitis in mice. *Gastroenterology.* **137:** 1795–1804.
5. Izumiya, Y., H. A. Bina, N. Ouchi, Y. Akasaki, A. Kharitonenkov, and K. Walsh. 2008. FGF21 is an Akt-regulated myokine. *FEBS Lett.* **582:** 3805–3810.
6. Hondares, E., R. Iglesias, A. Giralt, F. J. Gonzalez, M. Giralt, T. Mampel, and F. Villarroya. 2011. Thermogenic activation induces FGF21 expression and release in brown adipose tissue. *J. Biol. Chem.* **286:** 12983–12990.
7. Badman, M. K., P. Pissios, A. R. Kennedy, G. Koukos, J. S. Flier, and E. Maratos-Flier. 2007. Hepatic fibroblast growth factor 21 is regulated by PPARalpha and is a key mediator of hepatic lipid metabolism in ketotic states. *Cell Metab.* **5:** 426–437.
8. Inagaki, T., P. Dutchak, G. Zhao, X. Ding, L. Gautron, V. Parameswara, Y. Li, R. Goetz, M. Mohammadi, V. Esser, et al. 2007. Endocrine regulation of the fasting response by PPARalpha-mediated induction of fibroblast growth factor 21. *Cell Metab.* **5:** 415–425.
9. Gälman, C., T. Lundåsen, A. Kharitonenkov, H. A. Bina, M. Eriksson, I. Hafström, M. Dahlin, P. Amark, B. Angelin, and M. Rudling. 2008. The circulating metabolic regulator FGF21 is induced by prolonged fasting and PPARalpha activation in man. *Cell Metab.* **8:** 169–174.
10. Lundåsen, T., M. C. Hunt, L. M. Nilsson, S. Sanyal, B. Angelin, S. E. Alexson, and M. Rudling. 2007. PPARalpha is a key regulator of hepatic FGF21. *Biochem. Biophys. Res. Commun.* **360:** 437–440.
11. Reitman, M. L. 2007. FGF21: a missing link in the biology of fasting. *Cell Metab.* **5:** 405–407.
12. Uebanso, T., Y. Taketani, H. Yamamoto, K. Amo, S. Tanaka, H. Arai, Y. Takei, M. Masuda, H. Yamanaka-Okumura, and E. Takeda. 2012. Liver X receptor negatively regulates fibroblast growth factor 21 in the fatty liver induced by cholesterol-enriched diet. *J. Nutr. Biochem.* **23:** 785–790.
13. Archer, A., N. Venteclef, A. Mode, M. Pedrelli, C. Gabbi, K. Clément, P. Parini, J. Gustafsson, and M. Korach-André. 2012. Fasting-induced FGF21 is repressed by LXR activation via recruitment of an HDAC3 corepressor complex in mice. *Mol. Endocrinol.* **26:** 1980–1990.
14. Zhang, Y., Y. Xie, E. D. Berglund, K. C. Coate, T. T. He, T. Katafuchi, G. Xiao, M. J. Potthoff, W. Wei, Y. Wan, et al. 2012. The starvation hormone, fibroblast growth factor-21, extends lifespan in mice. *Elife.* **1:** e00065.
15. Guo, F., and D. R. Cavener. 2007. The GCN2 eIF2alpha kinase regulates fatty-acid homeostasis in the liver during deprivation of an essential amino acid. *Cell Metab.* **5:** 103–114.
16. Cheng, Y., Q. Meng, C. Wang, H. Li, Z. Huang, S. Chen, F. Xiao, and F. Guo. 2010. Leucine deprivation decreases fat mass by stimulation of lipolysis in white adipose tissue and upregulation of uncoupling protein 1 (UCP1) in brown adipose tissue. *Diabetes.* **59:** 17–25.
17. Cheng, Y., Q. Zhang, Q. Meng, T. Xia, Z. Huang, C. Wang, B. Liu, S. Chen, F. Xiao, Y. Du, et al. 2011. Leucine deprivation stimulates fat loss via increasing CRH expression in the hypothalamus and activating the sympathetic nervous system. *Mol. Endocrinol.* **25:** 1624–1635.
18. Zhang, Y., T. Lei, J. F. Huang, S. B. Wang, L. L. Zhou, Z. Q. Yang, and X. D. Chen. 2011. The link between fibroblast growth factor 21 and sterol regulatory element binding protein 1c during lipogenesis in hepatocytes. *Mol. Cell. Endocrinol.* **342:** 41–47.
19. Hansen, B. S., M. H. Vaughan, and L. Wang. 1972. Reversible inhibition by histidinol of protein synthesis in human cells at the activation of histidine. *J. Biol. Chem.* **247:** 3854–3857.
20. Hondares, E., M. Rosell, F. J. Gonzalez, M. Giralt, R. Iglesias, and F. Villarroya. 2010. Hepatic FGF21 expression is induced at birth via PPARalpha in response to milk intake and contributes to thermogenic activation of neonatal brown fat. *Cell Metab.* **11:** 206–212.
21. Díaz-Delfín, J., E. Hondares, R. Iglesias, M. Giralt, C. Caelles, and F. Villarroya. 2012. TNF-α represses β-Klotho expression and impairs FGF21 action in adipose cells: involvement of JNK1 in the FGF21 pathway. *Endocrinology.* **153:** 4238–4245.
22. Vilà-Brau, A., A. L. De Sousa-Coelho, C. Mayordomo, D. Haro, and P. F. Marrero. 2011. Human HMGCS2 regulates mitochondrial fatty acid oxidation and FGF21 expression in HepG2 cell line. *J. Biol. Chem.* **286:** 20423–20430.
23. Badman, M. K., A. Koester, J. S. Flier, A. Kharitonenkov, and E. Maratos-Flier. 2009. Fibroblast growth factor 21-deficient mice demonstrate impaired adaptation to ketosis. *Endocrinology.* **150:** 4931–4940.
24. Kharitonenkov, A., T. L. Shiyanova, A. Koester, A. M. Ford, R. Micanovic, E. J. Galbreath, G. E. Sandusky, L. J. Hammond, J. S. Moyers, R. A. Owens, et al. 2005. FGF-21 as a novel metabolic regulator. *J. Clin. Invest.* **115:** 1627–1635.
25. Hotta, Y., H. Nakamura, M. Konishi, Y. Murata, H. Takagi, S. Matsumura, K. Inoue, T. Fushiki, and N. Itoh. 2009. Fibroblast growth factor 21 regulates lipolysis in white adipose tissue but is not required for ketogenesis and triglyceride clearance in liver. *Endocrinology.* **150:** 4625–4633.
26. Dutchak, P. A., T. Katafuchi, A. L. Bookout, J. H. Choi, R. T. Yu, D. J. Mangelsdorf, and S. A. Kliewer. 2012. Fibroblast growth factor-21 regulates PPARγ activity and the antidiabetic actions of thiazolidinediones. *Cell.* **148:** 556–567.
27. Thiaville, M. M., Y. X. Pan, A. Gjymishka, C. Zhong, R. J. Kaufman, and M. S. Kilberg. 2008. MEK signaling is required for phosphorylation of eIF2alpha following amino acid limitation of HepG2 human hepatoma cells. *J. Biol. Chem.* **283:** 10848–10857.

28. Pan, Y. X., H. Chen, M. M. Thiaville, and M. S. Kilberg. 2007. Activation of the ATF3 gene through a co-ordinated amino acid-sensing response programme that controls transcriptional regulation of responsive genes following amino acid limitation. *Biochem. J.* **401:** 299–307.
29. Fisher, F. M., J. L. Estall, A. C. Adams, P. J. Antonellis, H. A. Bina, J. S. Flier, A. Kharitonenkov, B. M. Spiegelman, and E. Maratos-Flier. 2011. Integrated regulation of hepatic metabolism by fibroblast growth factor 21 (FGF21) in vivo. *Endocrinology.* **152:** 2996–3004.
30. Matthias, A., K. B. Ohlson, J. M. Fredriksson, A. Jacobsson, J. Nedergaard, and B. Cannon. 2000. Thermogenic responses in brown fat cells are fully UCP1-dependent. UCP2 or UCP3 do not substitute for UCP1 in adrenergically or fatty scid-induced thermogenesis. *J. Biol. Chem.* **275:** 25073–25081.
31. Fisher, F. M., S. Kleiner, N. Douris, E. C. Fox, R. J. Mepani, F. Verdeguer, J. Wu, A. Kharitonenkov, J. S. Flier, E. Maratos-Flier, et al. 2012. FGF21 regulates PGC-1α and browning of white adipose tissues in adaptive thermogenesis. *Genes Dev.* **26:** 271–281.
32. Handschin, C., and B. M. Spiegelman. 2006. Peroxisome proliferator-activated receptor gamma coactivator 1 coactivators, energy homeostasis, and metabolism. *Endocr. Rev.* **27:** 728–735.
33. Coskun, T., H. A. Bina, M. A. Schneider, J. D. Dunbar, C. C. Hu, Y. Chen, D. E. Moller, and A. Kharitonenkov. 2008. Fibroblast growth factor 21 corrects obesity in mice. *Endocrinology.* **149:** 6018–6027.
34. Xu, J., D. J. Lloyd, C. Hale, S. Stanislaus, M. Chen, G. Sivits, S. Vonderfecht, R. Hecht, Y. S. Li, R. A. Lindberg, et al. 2009. Fibroblast growth factor 21 reverses hepatic steatosis, increases energy expenditure, and improves insulin sensitivity in diet-induced obese mice. *Diabetes.* **58:** 250–259.
35. Muise, E. S., B. Azzolina, D. W. Kuo, M. El-Sherbeini, Y. Tan, X. Yuan, J. Mu, J. R. Thompson, J. P. Berger, and K. K. Wong. 2008. Adipose fibroblast growth factor 21 is up-regulated by peroxisome proliferator-activated receptor gamma and altered metabolic states. *Mol. Pharmacol.* **74:** 403–412.
36. Xu, J., S. Stanislaus, N. Chinookoswong, Y. Y. Lau, T. Hager, J. Patel, H. Ge, J. Weiszmann, S. C. Lu, M. Graham, et al. 2009. Acute glucose-lowering and insulin-sensitizing action of FGF21 in insulin resistant mouse models–association with liver and adipose tissue effects. *Am. J. Physiol. Endocrinol. Metab.* **297:** E1105–E1114.
37. Tseng, Y. H., A. M. Cypess, and C. R. Kahn. 2010. Cellular bioenergetics as a target for obesity therapy. *Nat. Rev. Drug Discov.* **9:** 465–482.
38. Cao, W., A. V. Medvedev, K. W. Daniel, and S. Collins. 2001. beta-Adrenergic activation of p38 MAP kinase in adipocytes: cAMP induction of the uncoupling protein 1 (UCP1) gene requires p38 MAP kinase. *J. Biol. Chem.* **276:** 27077–27082.
39. Cannon, B., and J. Nedergaard. 2004. Brown adipose tissue: function and physiological significance. *Physiol. Rev.* **84:** 277–359.
40. Wang, T., Y. M. Shah, T. Matsubara, Y. Zhen, T. Tanabe, T. Nagano, S. Fotso, K. W. Krausz, T. M. Zabriskie, J. R. Idle, et al. 2010. Control of steroid 21-oic acid synthesis by peroxisome proliferator-activated receptor alpha and role of the hypothalamic-pituitary-adrenal axis. *J. Biol. Chem.* **285:** 7670–7685.
41. Kim, K. H., Y. T. Jeong, H. Oh, S. H. Kim, J. M. Cho, Y. N. Kim, S. S. Kim, H. Kim, K. Y. Hur, H. K. Kim, et al. 2013. Autophagy deficiency leads to protection from obesity and insulin resistance by inducing Fgf21 as a mitokine. *Nat. Med.* **19:** 83–92.